Evaluation of metal supported ceria based solid oxide fuel cell fabricated by wet powder spray and sintering

Oishi, Naoki; Yoo, Yeong

National Research Council Canada

Conseil national de recherches Canada

Canada

Evaluation of Metal Supported Ceria Based Solid Oxide Fuel Cell Fabricated by Wet Powder Spray and Sintering

Naoki Oishi[z] and Yeong Yoo

Institute for Chemical Process and Environmental Technology, National Research Council Canada, Ottawa, Ontario K1A 0R6, Canada

A ceria based solid oxide fuel cell was fabricated onto a porous stainless steel support by sintering process. The metal supported cell was composed of a porous AISI430 support, a $Ni–Ce_{0.8}Y_{0.2}O_{1.9}$ anode, a $Ce_{0.9}Gd_{0.1}O_{1.95}$ electrolyte, and a $La_{0.6}Sr_{0.4}Co_{0.2}Fe_{0.8}O_3$ cathode. A cell was tested at 600°C for up to 2700 h on humidified argon balanced hydrogen and air. The cell showed no signs of degradation over 1200 h at low current densities of 0.16 and 0.24 A cm^{-2}; however, under a high current density of 0.32 A cm^{-2}, the cell voltage dropped by 25% in 1400 h. Impedance measurements showed a sharp increase in polarization resistance that could be associated with the cathode. Ohmic resistances from the oxide scale and electrodes did not significantly contribute to the overall resistance, while electrode polarization resistance accounted for more than half of the overall resistance.
© 2009 The Electrochemical Society. [DOI: 10.1149/1.3253653] All rights reserved.

The early development of metal supported solid oxide fuel cells (SOFCs) in the middle of the 1960s demonstrated that zirconia cells with a variety of porous metal supports made of nickel or stainless steel were operational at 710–800°C.[1,2] In the 1980s, nickel supported thin zirconia cells fabricated by vacuum evaporation and back-etch were reported to be operational at 500–700°C.[3-5] However, it was not until the 1990s that a couple of research organizations developed metal supported SOFCs with reasonable cell characteristics.[6-9] The metal support structure using a ferritic stainless steel material allowed for enhancement of the mechanical strength of cells, improving the redox stability of cell stacks and minimizing the usage of costly electrode and electrolyte materials.[10] In recent years, there has been an increasing number of research activities on metal supported SOFCs with ferritic stainless steel materials.[11-16]

It is important to establish inexpensive technologies for manufacturing to further reduce costs. In fabricating metal supported SOFCs, using conventional ceramic manufacturing technologies is advantageous from an economic perspective. The conventional ceramic technologies in producing ceramic bodies with powder materials include molding, pressing, and sintering, which are all affordable technologies. The range of thickness of cell components, i.e., the cathode, electrolyte, and anode, is projected to lie within 1–30 μm; therefore, wet powder spray technology[17,18] is considered one of the candidates for forming thin cell components on a support from a viewpoint of thickness controllability. By replacing the molding process in conventional ceramic manufacturing technologies with a spraying process, such ceramic manufacturing technologies can be exploited to make thin layers on a support.

The objective of this study is to fabricate stainless steel supported SOFCs by using such a modified ceramic manufacturing technology involving the wet powder spray and subsequent sintering step with an attempt to operate cells at a lower temperature of 600°C, to check their long-term stability, and to evaluate cell components based on electrical resistivity.

Experimental

Commercially available porous AISI430 stainless steel (Fe-17Cr) sheets made by powder metallurgy were used as a support. The porosity of the sheet was about 15%. A porous stainless steel support was prepared in a 25 mm diameter disk form, 1.2 mm thick. The porous supports were cleaned in organic solvents and passivated in nitric acid before fabricating cell structures on them.

A trilayer of anode, electrolyte, and cathode was fabricated as follows.[19] First, an anode layer was deposited onto the surface of a porous support by wet powder spray[17,18] using a colloidal suspension. The sprayed anode layer was pressed to have the sprayed surface smooth, and then prefired at 900°C for 1 h. Subsequently, an electrolyte layer was sprayed in a similar manner to the anode spray. After a binder burnout process at 500°C, the electrolyte layer was isostatically pressed at 345 MPa to achieve a high level of packing density and then sintered at 1050°C in a nonoxidizing atmosphere for 1 h. A cathode layer was finally attached by spraying and firing at 850°C for 3 h. Suspensions were prepared with an oxide powder, organic agents (binder and surfactant), and an alcohol medium. 55 wt % NiO–45 wt % $Ce_{0.8}Y_{0.2}O_{1.9}$ composite (Ni-CY82) was used for the anode material and $Ce_{0.9}Gd_{0.1}O_{1.95}$ (CG91) was used for the electrolyte. The cathode was $La_{0.6}Sr_{0.4}Co_{0.2}Fe_{0.8}O_3$ (LSCF6428). In this work, zirconium (0.5–1 cation %) was used as a sintering inhibitor for the anode for the purpose of keeping the anode layer porous during the electrolyte sintering, whereas iron (0.5–1 cation %) was used as a sintering aid[20] to densify the electrolyte layer.

To evaluate polarization resistances in the electrodes, impedance measurements were carried out in the temperature range 400–600°C on symmetrical cells: an LSCF6428 cathode | CG91 electrolyte | LSCF6428 cathode cell, and a Ni-CY82 anode | CG91 electrolyte | Ni-CY82 anode cell, with an excitation voltage of 10 mV over the frequency range 1×10^6 to 1×10^{-3} Hz. Electrodes were deposited by spray onto 13 mm diameter, 0.9 mm thick CG91 electrolyte disks. For anodes, due to technical difficulties in realizing the fabrication conditions similar to those for cell manufacturing, an anode layer was sprayed onto both sides of an electrolyte disk that was sintered at 1050°C, and then fired at the same temperature after pressing. In the cell manufacturing, the deposited anode, which was prefired at 900°C, was cofired with the electrolyte at 1050°C after pressing.

The cell fabricated on a porous stainless steel support was tested by using a galvanostat on humidified argon balanced hydrogen and air at 600°C. Fuel utilization was kept below 10%. A schematic diagram of the fuel cell test rig is shown in Fig. 1. The temperature was monitored underneath the porous support in the fuel atmosphere. In the cathode side, the surface of the Fe-17Cr stainless steel support was coated with either the CG91 electrolyte or ceramic cements so that there was no direct exposure to air (negligible chromium vapor species in the cathode). The current density was calculated based on the area of the cathode with a smaller diameter than the electrolyte. Impedance measurements were also performed during testing. After testing, microanalysis using a scanning electron microscope (SEM) was carried out on cross sections of a tested sample.
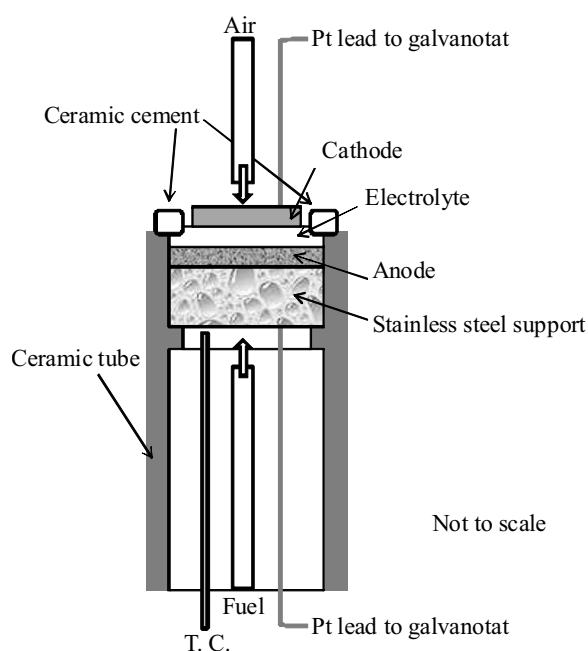
z E-mail: naoki.oishi@nrc-cnrc.gc.ca

Figure 1. Schematic diagram of a fuel cell test rig placed in a furnace.

Figure 3. Arrhenius plots of R_{pol} for the LSCF6428 cathode and the Ni-CY82 anode.

Results and Discussion

Estimation of polarization resistance by impedance measurements of symmetrical cells.— Impedance spectra (Nyquist plots) for the LSCF6428 cathode and the Ni-CY82 anode on CG91 electrolytes are shown in Fig. 2. Air was used as a cathode gas, and humidified argon balanced 50% hydrogen (wet Ar–50% H_2) was used as an anode gas. The impedance spectrum for LSCF6428 at 597°C is made of one arc with its peak at 3.3×10^3 Hz and an inductive response at high frequency, while at a low temperature two well-defined arcs are observed. Although two overlapping arcs at high frequency (peak at $\sim 10^3$ Hz) and low frequency (peak at ~ 10 Hz),

attributing the former to charge transfer and the latter to diffusion of oxygen species, are reported,[21,22] the low frequency arc is not distinguishable in this impedance spectrum. Like the LSCF6428, the impedance spectrum for Ni-CY82 at 597°C seems to consist of one distorted arc with its peak at 3.6×10^{-3} Hz and an inductive component, while at a low temperature there appears to be another arc at high frequency as well as a low frequency arc. Literature on impedance measurements for cermet anode–ceria electrolyte systems is limited; impedance spectra for copper or nickel cermet anodes on ceria electrolytes are reported to have a low frequency arc ($\sim 10^{-3}$ Hz).[23,24]

In this work, polarization resistance, R_{pol}, was defined by the difference in the two x-intercepts plotted or by fitting a semicircle to a low frequency arc in obtaining the length of the cord on the x-axis where two arcs were noticeable at low temperatures. Although impedance spectra in the temperature range tested contained inductance contributions, no calibration was made to eliminate the effect of inductance, e.g., at 597°C 0.84 Ω cm^2 for LSCF6428 and 0.05 Ω cm^2 for Ni-CY82. As shown in Fig. 3, Arrhenius plots of R_{pol} are linear, estimating activation energies at 1.7 eV for LSCF6428 and 1.0 eV for Ni-CY82 on CG91 electrolytes. Over the temperature range tested, the Ni-CY82 anode has at least 1 order of magnitude lower polarization resistance than the LSCF6428 cathode. There are many reports regarding the polarization resistance and activation energy of the $La_{0.6}Sr_{0.4}Co_{0.2}Fe_{0.8}O_3$ cathode–ceria electrolyte systems by using impedance spectroscopy;[21,22,25-28] however, polarization resistances are widely varied, especially in the temperature range 500–600°C where there is as much as 1 order of magnitude of difference at the same temperature, e.g., at 600°C from 0.3 to 4 Ω cm^2, while activation energies obtained on Arrhenius plots lie within a range of 1.1–1.7 eV. Compared with these, our estimated polarization resistance is relatively low, about 0.8 Ω cm^2 at 600°C with the activation energy being high (1.7 eV). Little is known on cermet anode–ceria electrolyte systems. The activation energy calculated for Ni-CY82 (1.0 eV) agrees with a value of 0.95–0.96 eV for a Ni–$Ce_{0.8}Sm_{0.2}O_{1.9}$ cermet anode on a $Ce_{0.8}Sm_{0.2}O_{1.9}$ electrolyte system characterized by a three-electrode configuration.[29] However, the reported polarization resistance is about 0.6 Ω cm^2 at 600°C, which is more than 1 order of magnitude higher than our obtained resistance (0.05 Ω cm^2). In this work, the firing temperature was lower, and isostatic pressing was
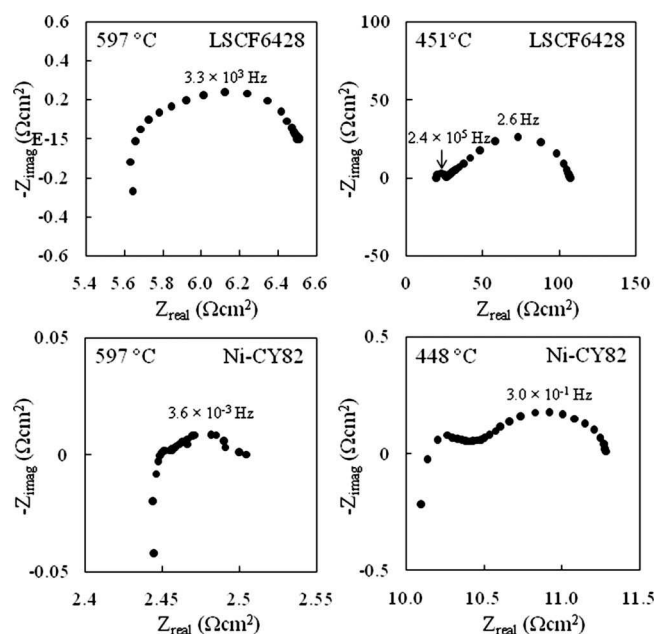

Figure 2. Impedance spectra (Nyquist plots) for the LSCF6428 cathode and the Ni-CY82 anode on CG91 electrolytes. The temperature and peak frequency are shown.
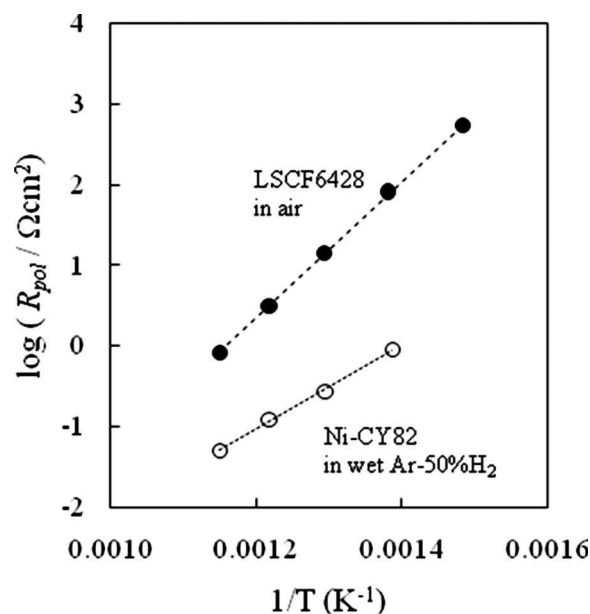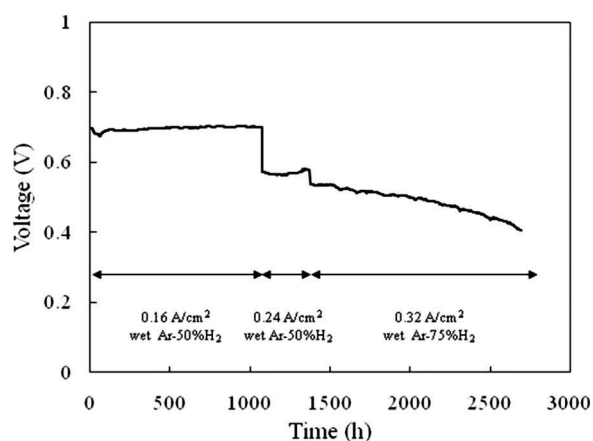
Figure 4. Voltage of a stainless steel supported ceria based cell at 600°C under different galvanostatic operations.

Figure 6. Impedance spectra at 600°C under open-circuit condition at different times. Hydrogen fuel concentration is shown in percent.

applied to improve the bonding between the electrolyte and the anode before firing; therefore, these processing conditions are thought to retain high surface area to provide lower polarization resistance.

Long-term testing of a cell fabricated on a porous stainless steel support.— A cell fabricated on a porous stainless steel support was about 20 μm in anode thickness, about 10 μm in electrolyte thickness, and about 25 μm in cathode thickness. Thicknesses were measured with the step height around the edge of each layer by an optical microscope. The density of the sintered electrolyte remained unclear due to variability in observed thickness; however, image analysis on surface SEM micrographs indicated a volume density of 96–98%. The open-circuit voltage, V_{oc}, was about 0.84 V at 600°C on wet Ar–50% H_2 and air.

Figure 4 shows the voltage change in a cell tested for up to 2700 h under different galvanostatic operations: 0.16, 0.24, and 0.32 A cm^{-2}. There is no noticeable voltage degradation for about 1200 h after 100 h during the 0.16 and 0.24 A cm^{-2} operations. After the current density was increased from 0.24 to 0.32 A cm^{-2}, the cell started to show voltage degradation over time, and the cell voltage dropped by 25% in the following 1400 h.

Current density–voltage characteristics taken at 20 and 1000 h during the 0.16 A cm^{-2} galvanostatic operation, at 1375 h during the 0.24 A cm^{-2} operation, and at 2100 and 2700 h during the 0.32 A cm^{-2} operation are shown in Fig. 5. During the 0.16 A cm^{-2} galvanostatic operation, V_{oc} remained the same, approximately 0.84 V, while the current density was slightly increased.
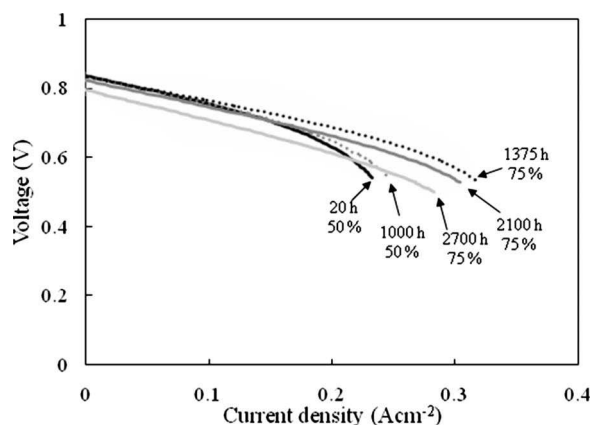

Figure 5. Current density–voltage characteristics at 600°C at different times. Hydrogen fuel concentration is shown in percent.
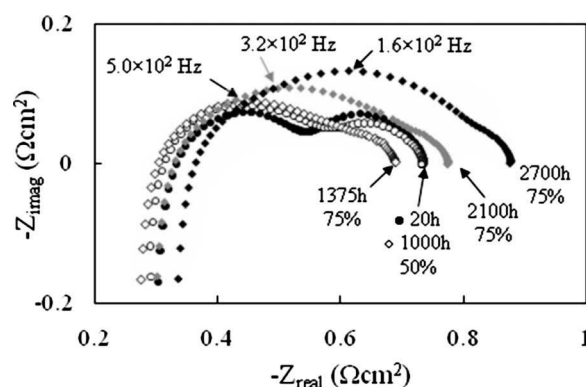
When the hydrogen concentration was changed from 50 to 75% at 1375 h, there appeared to be a great increase in current density with V_{oc} being almost similar. In our preliminary fuel cell test experiments at 600°C, V_{oc} was found to gradually increase with time when fuel started to be fed into the anode; in addition, high concentration fuel had an impact on the rate of V_{oc} generation, and it was therefore thought that the nickel oxide in the anode deposited onto such a thick porous support (1.2 mm) with a low porosity ($\sim$15%) is not readily reduced to increase porosity at 600°C. Accordingly, the increase in current density seen in Fig. 5 can be attributed to the improved diffusivity of H_2 and H_2O in the anode side, which is associated with concentration polarization. During the 0.32 A cm^{-2} galvanostatic operation from 1375 to 2700 h, V_{oc} as well as current density decreased.

Figure 6 shows the impedance spectrum under open-circuit voltage condition at different times. At 20 and 1000 h, the spectra are made of two arcs at high and low frequencies, which are similar in size. As expected from slopes near V_{oc} on the current density–voltage characteristics in Fig. 5, the overall resistance obtained from impedance measurements remained almost unchanged, about 0.73 Ω cm^2. The impedance spectrum at 1375 h on 75% H_2 has a smaller arc at low frequency than that at 20 and 1000 h measured on 50% H_2. In our separate work[30] using porous supports made by laser drilling, which could provide high gas permeability due to straight open pores in the thin (0.25 mm) support with high porosity (20%), the arc at low frequency was merged to the high frequency arc; therefore, the low frequency arc is thought to be associated with polarization in the anode side, especially concentration polarization (in anode and porous support). In fact, a cell fabricated on the laser-drilled porous support was found to deliver more current with good linearity with voltage until a high current density ($>$0.5 A cm^{-2}), which indicated the importance of gas transport in porous supports in decreasing concentration polarization. In contrast to the peak frequency of the arc for the symmetrical anode ($\sim$10^{-3} Hz) shown in Fig. 2, the impedance spectrum for the symmetrical cathode appeared to have an arc with its peak lying at a higher frequency, 10^3 Hz range; therefore, the high frequency arc with a peak at a range 10^2–10^3 Hz in the impedance spectrum for a cell is thought to have a correlation with cathode. After 1375 h, the arc at the high frequency seems to grow, with its peak frequency shifting toward the low frequency from 5.0 × 10^2 Hz at 1375 h to 1.6 × 10^2 Hz at 2700 h, and the overall resistance increases by 0.19 Ω cm^2. In the nickel–cermet anode supported zirconia cells tested for 1500 h at 750°C at various current densities, the high frequency arc is reported to increase with increasing current densities.[31] Compared to the change in the overall resistance, the ohmic resistance change is only 0.05 Ω cm^2, and high current density operation is found to deteriorate polarization resistance. Because the range of the high frequency arc observed on a cell under open potential is closer to
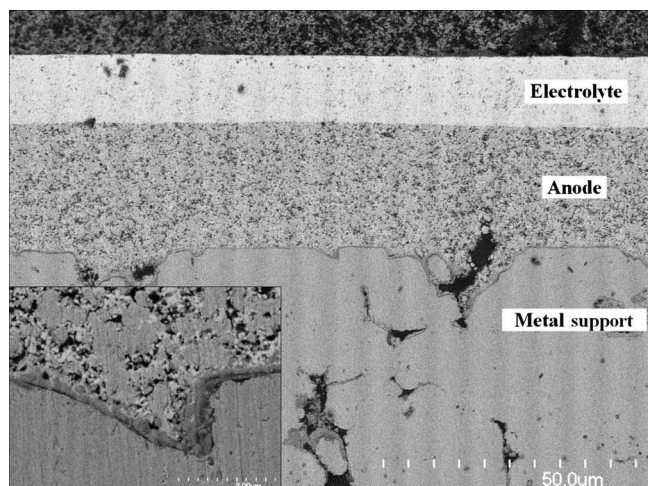
Figure 7. SEM micrograph of a cross section of a stainless steel supported ceria based cell tested at 600°C for 2700 h. The interface region between the stainless steel support and the Ni-CY82 anode is shown in the inset.

that of an arc observed on the cathode symmetrical cell, the high frequency arc is thought to reflect polarization in the cathode rather than polarization in the anode. The degradation under the 0.32 A cm^{-2} operation where the high frequency arc is growing in size is thought to be caused by some change in the cathode, which could also explain the drop in V_{oc} from 0.84 to 0.79 V due to increased electrode polarization.

Evaluation of resistive cell components.— The cross-sectional SEM micrographs of the cell tested for 2700 h are shown in Fig. 7. The thickness of the Ni-CY82 anode is 23–26 μm, and the CG91 electrolyte is 13–14 μm. Although the cathode is not shown due to partial delamination during sample preparation, the thickness range was 25–30 μm. A thermally grown oxide scale on the Fe–17Cr porous stainless steel support is seen (inset of Fig. 7), but in the stainless steel phase underneath the oxide scale, there is no continuous inner oxide phase like SiO_2.

Assuming that the oxide scale is made of pure Cr_2O_3, from the resistivity data for Cr_2O_3,[32] the area specific resistance of the oxide scale with a thickness of less than 0.5 μm is calculated to be less than 1×10^{-3} Ω cm^2 at 600°C. In general, AISI430 has manganese as a minor element (up to 1 wt %); therefore, the resistivity of the oxide scale can be decreased by manganese doping, which would be the case for this oxide scale grown. The electrical resistivity of the stainless steel is also negligible ($\ll 10^{-3}$ Ω cm^2).

Because the Ni-CY82 anode is estimated to have approximately 42 vol % nickel and 58 vol % $Ce_{0.8}Y_{0.2}O_{1.9}$, the matrix of this anode layer is made up of $Ce_{0.8}Y_{0.2}O_{1.9}$. Resistivity measurement of a sintered Ni-CY82 disk showed that it has a metallic behavior in the temperature range 550–650°C in wet Ar–50% H_2, and the resistivity at 600°C was about 1.9 Ω cm. The 23–26 μm thick anode layer is expected to be below 5×10^{-3} Ω cm^2 in area specific resistance.

According to earlier reports,[33,34] the total resistivity (lattice plus grain-boundary contributions) for $Ce_{0.9}Gd_{0.1}O_{1.95}$ is 62–70 Ω cm at 600°C in air, and the area specific resistance of a 13–14 μm thick electrolyte is calculated to be 0.08–0.1 Ω cm^2 in air. However, the resistivity of cerium oxide is decreased with decreasing oxygen partial pressure, p_{O_2}, due to the occurrence of electronic conductivity ($Ce^{4+} \rightarrow Ce^{3+} + e^-$). It is difficult to obtain the resistivity of a ceria electrolyte layer under a p_{O_2} gradient. The electrolyte layer may have a resistivity close to that of the anode. As can be roughly estimated from the impedance spectra of symmetrical cells by assuming that the lower x-axis intercept corresponds to the resistance of a ceria electrolyte disk, the resistivity in air is 125 Ω cm, while

the resistivity in wet Ar–50% H_2 is 50 Ω cm, which is less than half of the resistivity in air. Accordingly, the electrolyte's resistance would not exceed 0.1 Ω cm^2 in the form of a cell.

The resistivity of $La_{0.6}Sr_{0.4}Co_{0.2}Fe_{0.8}O_3$ is reported[35] to be 2.9 $\times 10^{-3}$ Ω cm at 600°C in air, and the area specific resistance of a 25–30 μm thick cathode is well below 1×10^{-5} Ω cm^2, assuming a porosity of 30%.

From the impedance spectrum at 20 h, ohmic and polarization resistances are 0.32 and 0.41 Ω cm^2, respectively. The ohmic resistances of the oxide scale, the anode, and cathode layers are low enough so that these components would not contribute significantly to the ohmic resistance in a cell. The electrolyte layer might well account for most of the ohmic resistance. However, the measured ohmic resistance of 0.32 Ω cm^2 appears to be greater than the estimate, less than 0.1 Ω cm^2; there needs to be some unknown resistive component, which is yet to be identified to explain this inconsistency. In contrast, the polarization resistance of 0.41 Ω cm^2 obtained on the impedance measurement under open-circuit voltage condition is less than half of the value of 0.89 Ω cm^2 that was compiled with the anode and cathode contributions (anode, 0.05 Ω cm^2 and cathode, 0.84 Ω cm^2) obtained on symmetrical cells. From a polarization point of view, the cell appeared to perform better than expected, while this cell did not perform as good as the expectation from an ohmic resistance perspective, but the cell was found to show characteristics better than expected; 0.73 Ω cm^2 on a cell over 0.99 Ω cm^2 based on estimates. Different from impedance measurements on symmetrical cells where there is no steady current except for a current responding to the applied signal voltage, during the impedance measurement under open-circuit voltage on a thin ceria based cell, there is a leak current due to its electronic conductivity; therefore, it is thought that the electrodes, especially the cathode, are already activated by its leak current, leading to a lower polarization resistance during the measurement.

In the cell configuration of the porous AISI430 stainless steel support, the Ni-CY82 anode, the CG91 electrolyte, and the LSCF6428 cathode, ohmic resistances from the oxide scale on the support, the anode, and the cathode have little impact on the overall resistance. It is not sufficient to explain the measured ohmic resistance by using the estimated electrolyte contribution. The polarization resistance is found to account for more than half of the overall resistance, and the polarization resistance is thought to be dominated by cathode.

Conclusions

A stainless steel supported SOFC was made by the wet powder spray and sintering route. The open-circuit voltage of a 13-14 μm thick ceria based cell was about 0.84 V at 600°C on humidified argon balanced 50% hydrogen and air. There was no noticeable voltage degradation over 1200 h under the 0.16 and 0.24 A cm^{-2} galvanostatic operations; however, under the 0.32 A cm^{-2} operation, the cell voltage dropped by 25% in 1400 h. Impedance measurements during the long-term test showed an increase in polarization resistance that could be associated with the cathode. In the stainless steel supported ceria based cells operated at 600°C, ohmic resistances from the oxide scale, anode, and cathode do not significantly contribute to the overall resistance, while polarization resistance, presumably mainly from the cathode, was found to account for more than half of the overall resistance.

Acknowledgments

References

1. K. R. Williams and J. G. Smith, U.K. Pat. GB1049428 (1966).
2. K. R. Williams and J. G. Smith, U.S. Pat. 3,464,861 (1969).

3. T. Namikawa, Y. Yamazaki, I. Saitoh, T. Kanai, S. Sumiya, and M. Sato, *Denki Kagaku oyobi Kogyo Butsuri Kagaku*, **52**, 714 (1984).
4. T. Ando, T. Namikawa, and Y. Yamazaki, *Denki Kagaku oyobi Kogyo Butsuri Kagaku*, **54**, 614 (1986).
5. T. Namikawa, T. Ando, H. Michibata, and Y. Yamazaki, *Denki Kagaku oyobi Kogyo Butsuri Kagaku*, **55**, 712 (1987).
6. T. Okuo, S. Nagata, Y. Kaga, Y. Kasuga, A. Momma, K. Tsukamoto, and F. Uchiyama, in *The First European Solid Oxide Fuel Cell Forum*, U. Bossel, Editor, Vol. 2, p. 909, European SOFC Forum Proceedings Series, Oberronhrdorf, Switzerland (1994).
7. S. Nagata, T. Okuo, Y. Kaga, Y. Kasuga, K. Momma, K. Tsukamoto, and F. Uchiyama, in *The Fourth International Symposium on Solid Oxide Fuel Cells*, M. Dokiya, O. Yamamoto, H. Tagawa, and S. C. Singhal, Editors, PV 95-1, p. 221, The Electrochemical Society Proceedings Series, Pennington, NJ (1995).
8. M. Lang, R. Henne, G. Schiller, and N. Wagner, in *The Fifth International Symposium on Solid Oxide Fuel Cells*, U. Stimming, S. C. Singhal, H. Tagawa, and W. Lehnert, Editors, PV 94-40, p. 461, The Electrochemical Society Proceedings Series, Pennington, NJ (1997).
9. G. Schiller, R. Henne, and M. Lang, in *The Fifth International Symposium on Solid Oxide Fuel Cells*, U. Stimming, S. C. Singhal, H. Tagawa, and W. Lehnert, Editors, PV 97-40, p. 635, The Electrochemical Society Proceedings Series, Pennington, NJ (1997).
10. P. Bance, N. P. Brandon, B. Girvan, P. Holbeche, S. O'dea, and B. C. H. Steele, *J. Power Sources*, **131**, 86 (2004).
11. T. Franco, Z. Ilhan, M. Lang, G. Schiller, and P. Szabo, in *The Ninth International Symposium on Solid Oxide Fuel Cells*, S. C. Singhal and J. Mizusaki, Editors, PV 2005-07, p. 344, The Electrochemical Society Proceedings Series, Pennington, NJ (2005).
12. Y. B. Matus, L. C. DeJonghe, C. P. Jacobson, and S. J. Visco, *Solid State Ionics*, **176**, 443 (2005).
13. C. Lee and J. Bae, *J. Power Sources*, **176**, 62 (2008).
14. M. C. Tucker, G. Y. Lau, C. P. Jacobson, L. C. DeJonghe, and S. J. Visco, *J. Power Sources*, **175**, 447 (2008).
15. R. Hui, J. O. Berghaus, C. Deces-Petit, W. Qu, S. Yick, J.-G. Legoux, and C. Moreau, *J. Power Sources*, **191**, 371 (2009).
16. S. Hui, D. Yang, Z. Wang, S. Yick, C. Deces-Petit, W. Qu, A. Tuck, R. Maric, and D. Ghosh, *J. Power Sources*, **167**, 336 (2007).
17. K. Wippermann, U. Stimming, H. Jansen, and D. Stover, in *The Third International Symposium on Solid Oxide Fuel Cells*, S. C. Singhal and H. Iwahara, Editors, PV 93-4, p. 180, The Electrochemical Society Proceedings Series, Pennington, NJ (1993).
18. R. Wilkenhoner, W. Mallener, H. P. Buchkremer, T. Hauber, and U. Stimming, in *The Second European Solid Oxide Fuel Cell Forum*, B. Thorstensen, Editor, p. 279,

European SOFC Forum Proceedings Series, Oberronhrdorf, Switzerland (1996).
19. N. Oishi, Y. Yoo, and I. Davidson, *ECS Trans.*, **7**(1), 781 (2007).
20. C. Kleinlogel and L. J. Gauckler, in *The Sixth International Symposium on Solid Oxide Fuel Cells*, M. Dokiya and S. C. Singhal, Editors, PV 99-19, p. 225, The Electrochemical Society Proceedings Series, Pennington, NJ (1999).
21. J. A. Lane, P. H. Middleton, H. Fox, B. C. H. Steele, and J. A. Kilner, in *The Second International Symposium on Ionic and Mixed Conducting Ceramics*, T. A. Ramanarayanan, W. L. Worrell, and H. L. Tuller, Editors, PV 94-12, p. 489, The Electrochemical Society Proceedings Series, Pennington, NJ (1994).
22. V. Dusastre and J. A. Kilner, *Solid State Ionics*, **126**, 163 (1999).
23. S. Baron, N. Brandon, A. Atkinson, B. Steele, A. Bauen, and D. Hart, in *The Fifth European Solid Oxide Fuel Cell Forum*, J. Huijsmans, Editor, Vol. 1, p. 499, European Fuel Cell Forum Proceedings Series, Oberronhrdorf, Switzerland (2002).
24. E. Ramirez-Zabrera, A. Atkinson, N. Brandon, and B. Steele, in *The Fifth European Solid Oxide Fuel Cell Forum*, J. Huijsmans, Editor, Vol. 1, p. 531, European Fuel Cell Forum Proceedings Series, Oberronhrdorf, Switzerland (2002).
25. J. A. Lane, S. Adler, P. H. Middleton, and B. C. H. Steele, in *The Fourth International Symposium on Solid Oxide Fuel Cells*, M. Dokiya, O. Yamamoto, H. Tagawa, and S. C. Singhal, Editors, PV 95-1, p. 584, The Electrochemical Society Proceedings Series, Pennington, NJ (1995).
26. D. Waller, J. A. Lane, J. A. Kilner, R. J. Chater, P. S. Manning, and B. C. H. Steele, in *The Second European Solid Oxide Fuel Cell Forum*, B. Thorstensen, Editor, Vol. 2, p. 737, European Fuel Cell Forum Proceedings Series, Oberronhrdorf, Switzerland (1996).
27. J.-M. Bae and B. C. H. Steele, *Solid State Ionics*, **106**, 247 (1998).
28. J. M. Ralph, C. Rossignol, and R. Kumar, *J. Electrochem. Soc.*, **150**, A1518 (2003).
29. S. Wang, T. Kato, S. Nagata, T. Honda, T. Kaneko, N. Iwashita, and M. Dokiya, in *The Fourth European Solid Oxide Fuel Cell Forum*, A. J. McEvoy, Editors, Vol. 2, p. 479, European Fuel Cell Forum Proceedings Series, Oberronhrdorf, Switzerland (2000).
30. N. Oishi and Y. Yoo, *ECS Trans.*, **25**(2), 739 (2009).
31. A. Hagen, R. Barfod, P. V. Hendriksen, Y.-L. Liu, and S. Ramousse, in *The Ninth International Symposium on Solid Oxide Fuel Cells*, S. C. Singhal and J. Mizusaki, Editors, PV 2005-07, p. 503, The Electrochemical Society Proceedings Series, Pennington, NJ (2005).
32. A. Holt and P. Kofstad, *Solid State Ionics*, **100**, 201 (1997).
33. T. Kudo and H. Obayashi, *J. Electrochem. Soc.*, **123**, 415 (1976).
34. S. Wang, T. Kobayashi, M. Dokiya, and T. Hashimoto, *J. Electrochem. Soc.*, **147**, 3606 (2000).
35. L. W. Tai, M. M. Nasrallah, H. U. Anderson, D. M. Sparlin, and S. R. Sehlin, *Solid State Ionics*, **76**, 273 (1995).